

Supporting Information

Photoelectrochemical measurements

The electrochemical properties were measured in an electrochemical workstation (CHI 760D, CH Instruments, Inc.) via a conventional three-electrode system with a Pt plate electrode and an Ag/AgCl electrode (in saturated KCl) as the counter electrode and the reference electrode, respectively. The working electrodes were prepared by dropping the as-prepared catalyst slurry onto the fluorine-doped tin oxide (FTO) glass electrode and dried at room temperature. The working area of the working electrode was calibrated as 1.0 cm × 1.0 cm. 0.5 mol/L of Na₂SO₄ was used as the electrolyte solution.

Photocatalyst performance

Photocatalytic degradation of MO

The photocatalytic experiments for MO removal were conducted with a 150 W iodine tungsten lamp located 20 cm away from the photocatalytic system. All the tests started at room temperature (25 ± 1 °C). In a typical experiment, 50 mg of photocatalyst was dispersed in 50 mL of MO solution (10 mg/L) in a quartz tube by ultrasonication for 6 min and stirred at 900 r/min continuously for 30 min before light irradiation. After the lamp was switched on, 5 mL of the suspension were withdrawn at given time intervals and filtered with a syringe filter (polyethersulfone (PES) membrane, pore size 0.2 μm, filter diam. 13 mm (Sigma)) to remove the dispersed catalyst. Finally, the residual concentration of MO was measured by a UV-vis spectro-photometer at 465 nm.

Photocatalytic gas-solid CO₂ reduction

The photo-reduction of CO₂ was performed in a 50 mL glass solid-gas reactor system. In order to make the catalyst suitable for the reaction system, 30 mg of the catalyst was dispersed in 5 mL of deionized water by using ultrasonic treatment for 10 min. The dispersion was poured into a watch glass with a diameter of 3 cm, and dried in an

oven at 60°C. During the measurement process, 1 mL of DI water was put onto the bottom of a stainless-steel reactor, and then the watch glass with catalyst was set into the reactor. The reaction system was purged with pure CO₂ gas and vacuum treated twice to remove the air and impurities. Afterwards, the reactor was filled with CO₂ at a pressure of 2 atmospheres. The photocatalytic reaction was conducted under light irradiation (300 W xenon lamp, wavelength > 420 nm; the distance between the lamp and the watch glass was 18 cm; the central light power was 80 mW/cm²). The photocatalytic reaction was generally performed for 1 h before the objective products were collected with extraction syringes and estimated by GC-2080 gas chromatography (Ruipeng, China).

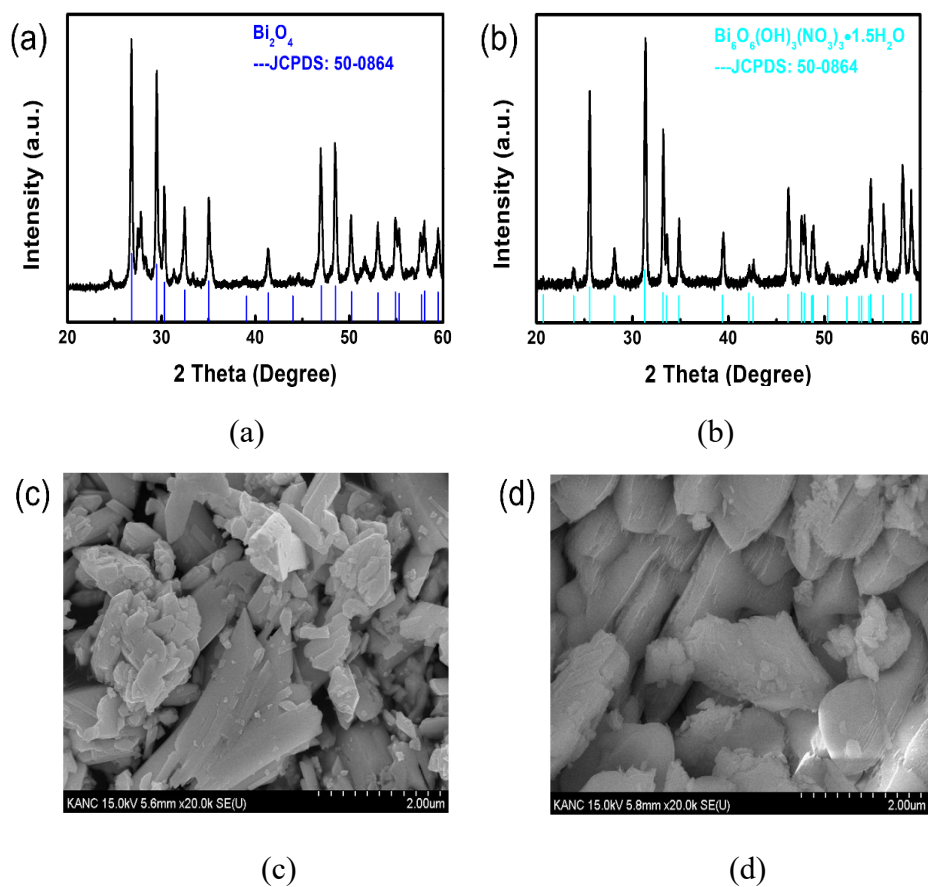
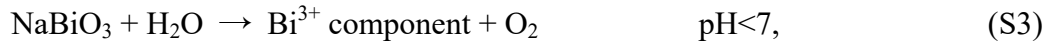


Fig. S1 XRD patterns and SEM images of the pH dependent samples at a reaction time of 12 h.

(a) XRD pattern at pH=7; (b) XRD pattern at pH<7; (c) SEM image at pH=7; (d) SEM image at pH<7.

To investigate the phase transition process affected by pH during hydrothermal reaction, neutral and acid environments were applied to make a comparison. After hydrothermal reaction for 12 h, the as-prepared samples were measured by XRD and SEM as shown in Fig. S1, yielding obviously different results. Rod like Bi₂O₄ and plate like Bi³⁺ components were formed in a neutral environment and acid environment, respectively. Obviously, the alkaline environment should be the key role to produce a rich oxygen vacancy containing the phase of BiO_{2-x}. In the case of strong oxidant of NaBiO₃, according to Nernst Equations, a lower pH could accelerate the redox reaction of conversing Bi⁵⁺ to Bi³⁺ while a high pH could suppress the degree of Bi⁵⁺/Bi³⁺ conversion. This could be the reason for different products with respect to various pH. The hydrothermal reaction process in different pH values and a certain temperature can be expressed with Eqs. (S1)–(S3).



Thereby, it is possible to produce other Bi-component composites by adjusting the reaction pH, time, and temperature.

Table S1 Elemental ratios measured by XPS for NB-*x*.

Element	NB-0	NB-3	NB-6	NB-12	NB-16	NB-21
	/(Atomic fraction, %)	/(Atomic fraction, %)	/(Atomic fraction, %)	/(Atomic fraction, %)	/(Atomic fraction, %)	/(Atomic fraction, %)
O	48.01	49.79	488.88	54.82	55.87	56.36
Na	20.39	16.81	14.24	3.45	2.54	2.63
Bi	31.61	33.41	36.88	41.73	41.59	41
Total:	100.00	100.00	100.00	100.00	100.00	100.00
Atomic ratio	1.52	1.49	1.32	1.31	1.34	1.37

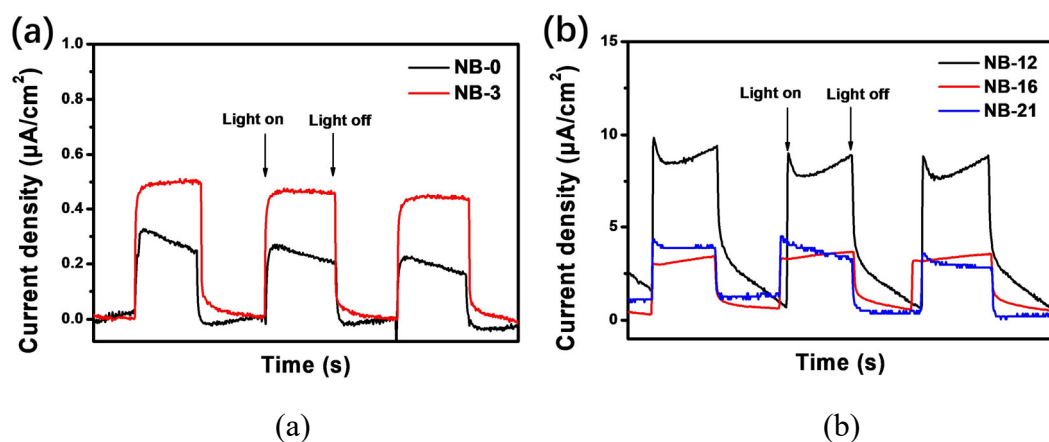


Fig. S2 Comparison of photocurrent densities under simulated sunlight (1 sun).
(a) NB-0 and NB-3; (b) NB-12, NB-16 and NB-21.

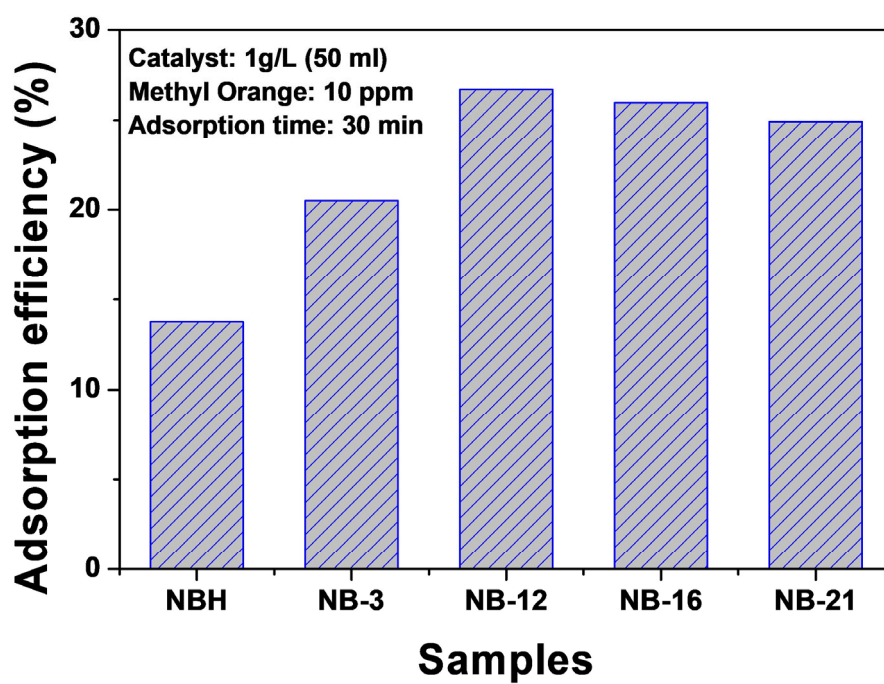
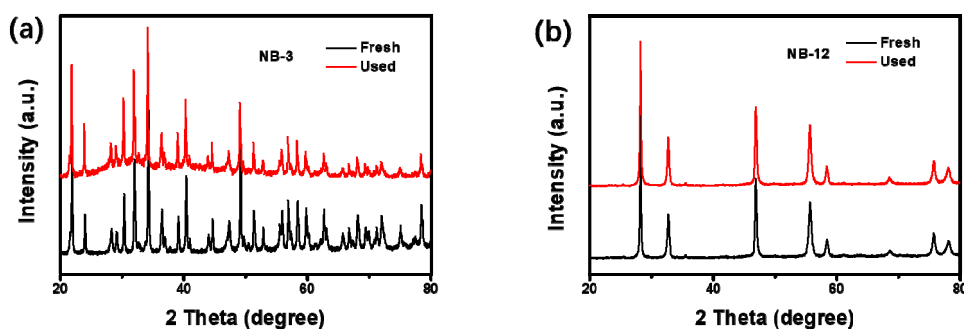


Fig. S3 Adsorption capacities of NB-0, NB-3, NB-12, NB-16, and NB-21 to MO in the equilibrium step in darkness.



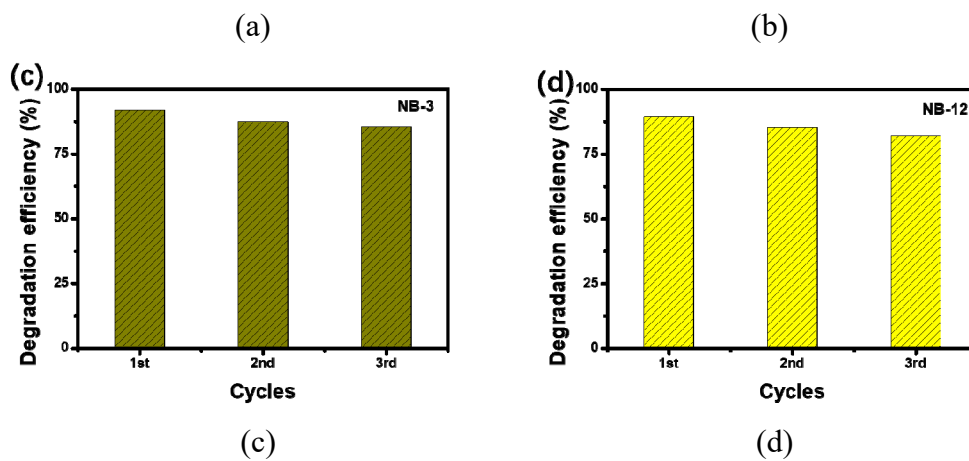


Fig. S4 Stability tests of NB-3 and NB-12 samples.

(a) XRD patterns of fresh and used samples of NB-3; (b) XRD patterns of fresh and used samples of NB-12; (c) recycle experiments of samples NB-3; (d) recycle experiments of samples NB-12.